Application of Shear Thickening Fluids on Soft Body Armor

2022-2023

Garrett Kawaguchi, Ethan Cam, Joseph Baur, Benjamin Lopez

Advisor:

Department of Mechanical Engineering:

Dr. Brian Ramirez

A Research Project

for the Learn Through Discovery Projects Hatchery

at California State Polytechnic University, Pomona

Project Summary

Body armors that are rated at NIJ level III must be able to stop a 7.62 NATO projectile, a full-size rifle cartridge. These projectiles can impart nearly 3500 joules and the materials used protect the wearer are typically “hard” armors that use steel, ceramic, or rigid composite plates. These variants tend to be expensive, heavy, and less flexible when compared to “soft” armors which use high tensile strength fibers as their main protective component. Currently, only a select few available soft body armors are rated for NIJ level III, all of which are of comparable thickness to their hard armor counterparts, which diminishes the advantages of soft armor, being lightweight and flexible. The results from this project aim to benefit military and law enforcement personnel, and civilians interested in an extra level of protection by providing insight into a less cumbersome alternative to contemporary body armor. Present and ongoing research has shown that shear thickening fluid (STF) infused fabrics have significantly increased energy absorption characteristics, however, these experiments are mostly focused on stab resistance and ballistic protection against pistol caliber cartridges. So far, an experiment that confirms the plausibility of an STF soft body armor capable of stopping full-power rifle cartridges has yet to be conducted. This project seeks to complete the aforementioned objective by developing a selection of fumed-silica-based STFs and studying their viscous properties. After which, they will be infused into Kevlar fabric and subjected to quasistatic and dynamic impacts. At the same time, it will be verifying some of the experimental results of other research papers pertaining to STFs.

Table of Contents

1.0 Introduction

Body armors used by the U.S. Army are mainly designed to protect from bullets, shrapnel, and stab threats to vital areas. Although the Army does not require that their armors be tested to NIJ (National Institute of Justice) standards, Figure 1, the current base version of the

Figure 1: The chart displays all NIJ ratings for body armors and the cartridges, at a specific velocity, that they are certified to protect the wearer from [1].

IOTV (Improved Outer Tactical Vest), weighing 3.6 pounds, wouldn't even qualify at NIJ Level IIA, the lowest available designation, as it is only rated to stop a 9mm, 124-grain projectile, traveling at 1,400 feet per second. Additional ceramic plate inserts are usually added to the front and rear of the torso plate carrier to increase the protective rating up to level 4, the highest available designation, allowing it to withstand full-power armor-piercing rifle rounds. Other armor modules can be added to further increase the coverage of the armor system to the extremities, however, this increased protection comes at a cost. When fully outfitted a size medium IOTV body armor system weighs 30 pounds.

The main advantages to soft body armors made from high-tensile strength fabrics such as Kevlar® or UHMWPE (ultra-high molecular weight polyethylene) are that they are lightweight and flexible. This allows the wearer to maintain their mobility as well as alleviate some of the fatigue concerns. They are also generally easier to manufacture and are significantly lighter than

either steel or ceramic armors. It is for these reasons that they are often favored, but in order for these fabrics to be able to stop higher impacting energy threats they must be stacked between 20-40 layers thick [1]. With this many woven layers, the advantages that a soft body provides are diminished and the products are still bulky and heavy pieces of equipment that restrict the wearer.

Currently available soft body armors that attempt to provide adequate ballistic protection without compromising on the benefits of high-strength fabrics are most often rated at Level IIIA. This rating provides resistance against some larger and higher impact energy pistol calibers but stops before any full-power rifle or intermediate rifle calibers. The step from level IIIA to level III exhibits an increase in impact velocity of 1,350 feet per second and marks the start of ballistic protection against full-power rifle cartridges (Figure 1). This jump leaves a rather large gap that is, for the most part, unaddressed. While there exists a few available soft body armors that possess special certifications for protections against intermediate rifle calibers such as the 5.56 NATO and the 7.62x39 mm, these models provide questionable advantages in the way of weight, flexibility, and cost over hard armors offering equal protection [3], 4, [5].

For these reasons, STF (shear thickening fluids) impregnated fabrics have been a topic of research since the early 2000s. This study seeks to experiment with silicone carbide, tungsten, and super-activated carbon STFs paired with Kevlar® in order to evaluate their potential use as level III soft body armors. A rheological test of the STFs, performed at three different temperatures, will be used to analyze the initial, critical, and peak viscosities through a range of shear rates. The STF-infused Kevlar® samples will then be subjected to a quasi-static piercing test, dynamic impact test, stab test, and high-velocity ballistic test to observe differences in failure modes as well as gain information about the energy absorption characteristics of the STF fabrics.

2.0 Literature Review

2.1 Shear Thickening Mechanisms

STFs (shear thickening fluids) are those that exhibit an increase in viscosity with increasing shear rate or shear stress. In colloidal dispersions a discontinuous shear thickening behavior, where the viscosity sharply increases, is observed above a critical shear rate [6]. The mechanism behind this phenomenon is theorized to be the collective contribution of many different interactions, however, the primary contributor is most often credited to the hydro clustering effect [7]. In previous years industrial processes considered the shear thickening behavior as a problem, clogging and jamming equipment which limited the movement speed of machinery. But in the early 2000s, the application of this problem as a solution to improved ballistic performance was brought to light [8]. By intercalating high-tensile strength fabrics with STFs their ability to withstand greater threats was realized.

As previously mentioned STFs, or dilatants, are non-Newtonian fluids that experience an increase in viscosity with an increase in shear rate. Typically, STFs are composed of two main constituents: nano or micro-sized dispersed particles and a carrying fluid medium. The process of shear thickening is reversible where the absence of shear forces allows the fluid to flow. With small particles, Van der Waals forces dominate the fluid behavior at equilibrium [6]. Increasing the shear rate to a critical value where the shear forces begin to overcome intermolecular forces and transition the particles to a mobile state before aggregating to display a shear thickening effect

(Figure 2). Granular suspensions, crosslinked polymers, micelle, and insoluble polymers are the four main categories of STFs [9]. Because of the variety of the systems and the way each of them displays shear thickening behavior the causes of shear thickening are not yet entirely understood. However, there are several theories that have been postulated to help explain how shear thickening occurs.

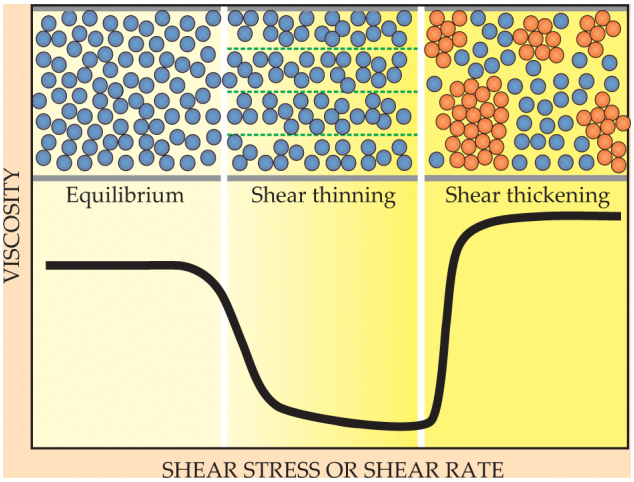

Figure 2: Schematic representation of shear thickening [11]

One of the traditional explanations often used is the order-disorder transition (ODT) theory. Proposed by Hoffman, it suggests that at low shear rates an STF does not exhibit shear thickening behavior [10]. Instead, the particles arrange themselves into ordered layers (one to several particles in thickness) and as the shear rate increases to a critical value the lamellae destabilize and collapse to form a disordered structure. At this point, the viscosity of the fluid increases in a disjunct manner.

Hydro-clustering is another theory that is given a significant share of credit for the cause of shear thickening. At very low shear rates the system can accommodate particle movement and the viscosity value is small. As the shear stress between the particles is increased and begins to overcome the intermolecular forces shear thinning is observed. At the critical shear rate, shear forces completely dominate the intermolecular forces which promote the formation of unstable

hydro-clusters. These aggregates cause a large increase in the viscosity of the fluid, but as soon as the shear stress is withdrawn, they rapidly return to their original undisturbed state via intermolecular forces and Brownian motion [9].

The jamming theory is most often used to describe solutions where the particle size exceeds four micrometers. In this size range the Brownian and intermolecular forces are not as present and contact between particles is much greater. As described by Olsson and Teitel a solution that exhibits jamming shows a sharp, discontinuous increase in viscosity of several orders of magnitude due to particles forming dispersed aggregates that propagate under shear stress which further blocks the flow of other particles [12]. When the volume fraction of the dispersed particles meets a high enough value, this eventually leads to a solution that is completely unable to flow [6].

Friction contact theory was proposed to bridge the gap between continuous and discontinuous shear thickening behavior. At low shear rates, the normal forces between the particles are low and the fluid lubrication forces have a significant effect on the low viscosity of the fluid. At high shear rates, the lubricating layer is destroyed leading to an increase in the contact and frictional force between the particles [13].

2.2 Shear Thickening Fluid Composition

STFs are colloidal mixtures primarily composed of two parts, a carrier fluid, and a dispersed insoluble particle. The carrier fluid acts as a dispersing medium between the particles, linking them together as well as facilitating the impregnation process into the fabric. Many studies concerned with ballistic protection through the use of STFs use fumed silica as the main dispersed particle, and PEG (polyethylene glycol) as the carrier fluid.

PEG is often chosen as a carrier fluid over water and other solvents due to its thermal stability, non-toxicity, biocompatibility, and ability to wet the chosen fabric moderately for impregnation, [8, 13, 15]. Ethanol is used as well in the creation of shear thickening fluids as a surfactant and a dilutant. When added to the carrier fluid, it reduces the shear thickening behavior during mixing with the particles. In addition to this, its properties as a surfactant allow the diluted shear thickening fluid to be impregnated into the fabric more effectively and can later be evaporated without changing the intended properties of the STF.

To create an STF that can effectively intercalated, particles on the order of 500nm or less are used. At this scale, the size of the particles is equal to or smaller than individual fibers allowing them to be absorbed and held by the fabric [9]. Fumed silica (SiO_2) nanoparticles are often chosen as the primary dispersed particle in the STF fluid due to its stability in an aqueous solution. When submerged, the silica becomes covered in a layer of silanol groups (SiOH). At its isoelectric point, the silica has a neutral net surface charge. Here, one alcohol molecule has the potential to bond to two silanolic hydrogens at the same time. With this configuration, the silica then behaves as a lyophilic colloid, due to the strong hydrated surface that is formed. This behavior is ideal for STFs, as it creates a stable and strongly bonded mixture [13].

The addition of other nanoparticles to a SiO_2 base has been found to increase the strength of the resulting shear-thickening fluid. Silicon carbide, for one, has been shown to improve the ballistic resistance of a shear-thickening fluid when used in conjunction with fumed silica nanoparticles. Although silicon carbide does not exhibit shear thickening behavior by itself, it has been proven to be an effective strengthening addition to the mixture [16].

2.3 Application of STFs on Body Armor

Several studies have been conducted showing the merits of the use of STFs on high strength fabrics. The unique properties of STFs can potentially allow soft body armors to maintain their advantages of over hard armor alternatives due to their flexibility remaining largely unhindered while the coefficient of friction between adjacent yarns is increased. This has the effect of enhanced energy absorption characteristics.

Drop tower and low velocity ballistic tests performed on STF-fabrics demonstrate a severe coning effect, implying increased involvement of secondary yarns. Data from these experiments also show a decrease in the back face signature deformation of a clay block. Together, these results indicate that the STF fabrics can more effectively disperse and transfer energy to adjacent yarns, spreading the force of impact over a greater area [8, 15]. The study from Mawkhlieng et al. realized a 133% enhancement for their VHMAP (very high modulus aromatic polymer) samples, further highlighting one of the benefits of STFs [15]. The ability to disperse impact energy in body armor is also a much-desired trait since the internal organs can still experience significant trauma even when the projectile is successfully stopped.

The hypothesis of increased yarn friction due to the intercalation of an STF within a fabric was confirmed by the results of Cwalina et al., in which various arrangements of Kevlar and Nylon were studied. The stab and puncture tests conducted reaffirm the above and add that the windowing effect of the STF fabric is reduced when met with an impact event that exceeds the critical shear rate [4]. A study conducted by Egres et at., 2005 also treated a stack of Kevlar with a silica based STF and found that its puncture and stab resistance was much greater than the neat Kevlar (untreated) sample using 20% fewer layers [17]

Investigations on which substances contribute the most to improvement of energy absorption and dissipation were carried out by Eric et al. by comparing the penetration resistance of neat Kevlar, dry silica impregnated Kevlar, ethylene glycol impregnated Kevlar, and STF impregnated Kevlar. The results showed that neither the dry silica nor ethylene glycol impregnated Kevlar samples could offer near the same energy absorption characteristics as the STF impregnated Kevlar, proving that only the combined effects of all components can produce the desired effects [8].

To determine the detriments to flexibility the STF impregnation process might have on flexibility of the fabrics cantilever tests have been performed on different forms of Kevlar and Nylon, both dry and STF infused. The findings compared the bend angles that were produced when a weight was hung off the edge of each specimen and showed that there was negligible change across all subjects [8, 15].

In terms of add-on weight incurred by the impregnation process, the addition can be significant. Wang conducted a study that explored the effects of differing amounts of STF add-on to Kevlar. The results showed that past an STF add-on weight ratio to fabric material of 1:1 there was very little improvement to any of the desirable characteristics [7]. This effectively means that in order to achieve the greatest enhancement to ballistic and stab resistance the weight of the neat material will be doubled.

2.4 Fabrics used in Soft Body Armors

The role of the fabric in soft body armor is to absorb the energy from a projectile while resisting penetration through the fabric and reducing the amount of localized deformation on the back side of the armor. The industry standard for military and police soft body armors since DuPont® developed the first Kevlar® vest in 1976 has been fabrics made of neat (containing no shear thickening fluids) p-aramid fibers [18]. Since p-aramid fabrics (Kevlar®, Twaron®, Technora®, Heracron®, etc.) are the industry standard and commercially available, the majority of research that has been done on the effects that STFs have on the energy absorption characteristics of ballistic fabrics have focused on these types of fabrics. While a number of studies have been performed on UHMWPE (Dyneema®, Spectra®, etc.) fabrics in conjunction with STFs, it pales in comparison to the work that has been done in regard to p-aramid fabrics. Outside of these two fabrics little research has been done on other promising materials such as Poly-hydroquinone Di-imidazopyridine (PIPD) (M5®) fabrics.

2.5 Material Dependent Parameters of Ballistic Fabrics

Tenacity, the tensile strength of a fiber with respect to its linear density, plays a vital role in the strength of a ballistic fabric, but it is not the only parameter to seek in an ideal fabric. While some fibers show tremendous strength to weight ratios, they may not be suitable for the use in soft body armors due to characteristics such as suffering from either elastic or brittle failure [1]. For this reason, the percentage of elongation before fracture is a critical parameter in the selection or fabrication of a ballistic fiber. If a fiber is too brittle, rather than transferring the load to other fibers, it fractures locally, allowing the projectile to penetrate the layer of fabric. On the other hand,

if a fabric is too elastic, energy transfer from fiber to fiber is delayed, allowing for the back face of the body armor to stretch and cause undesirable localized deformation into the wearer.

Additionally, materials with a higher Young's modulus, the stiffness of a material, are preferred over those that are less rigid. Since the fibers in a soft body armor can be thought of net of long springs loaded in tension, the advantages of a stiffer fiber become clear. While a less rigid material may still be able to stop a projectile from penetrating through the armor, it will not transfer as much energy to the surrounding armor as a rigid fiber would (assuming no fracture), and ultimately leading to unacceptable levels of back face signature.

Since efficient transfer of energy from a fiber to surrounding fibers is beneficial to the function of body armor, higher inter-fabric frictional coefficients are preferred. With higher frictional forces between individual fibers, loads can be transferred between fibers more uniformly. Higher frictional forces within the weave of a fabric and between two layers of a fabric additionally reduce the overall flexibility of the soft body armor. While this has its disadvantages to the wearer's comfort, it has the benefit of reducing the back face signature of the armor.

Resistance to degradation of a material in its operational environment in the selection process needs to be carefully considered, and if a material is selected that does suffer from environmental degradation, its mode of failure needs to be understood at the very least. Kevlar fibers for example can lose up to 25% of their strength from as little as two days of ultra-violet exposure. Additionally, Zylon® a Poly P-phenylene Benzobisoxazole (PBO) fiber which had promising mechanical properties, was found to be prone to both hydrolytic and photolytic degradation. This understanding of Zylon® was only developed after studies were performed in light of controversy surrounding the efficacy of this ballistic fabric. This study resulted in Zylon®

being pulled from the market as a ballistic fabric and the recalling of all soft body armors manufactured with Zylon®.

2.6 Material Independent Parameters of Ballistic Fabrics

Outside of inherent material properties unique to each type of fiber, the structure of the ballistic fabrics and the layer stacking order of soft armors has been an area of interest.

Crimp is a measure of how much a yarn deviates from a straight line to necessitate weaving with perpendicular strands. When crimp exists in a yarn that is absorbing a perpendicular impact, all of the crimp must be pulled out of the yarn before it can carry high tensile loads. Fabrics with excessive crimp suffer from the same undesirable characteristics of fabric that have a low tensile modulus by allowing more localized deformation on the back face of a soft body armor. Since some crimp is inherent in two- and three-dimensional weaves, it is important to reduce the crimp necessary when selecting a weave pattern. Studies have shown that unidirectional fabrics, fabrics in which 75% - 90% of fibers run parallel and thus have little crimp, can give promising results in reducing the back face signature [1], [19].Two- and three-dimensional fabrics do have certain advantages over unidirectional fabrics. Two-dimensional fabric benefits from uniform mechanical properties and higher flexibility and comfort since they do not require the resin bonding that unidirectional fabrics do. Three-dimensional weaves have shown improvements in tensile strength over two-dimensional fabrics while still remaining resin free. Lastly, weave density, how tightly a fabric is woven, has an influence on overall strength. A tighter weave tends to damage fibers during manufacturing and too loose of weave increases the amount of undesirable crimp in the fabric.

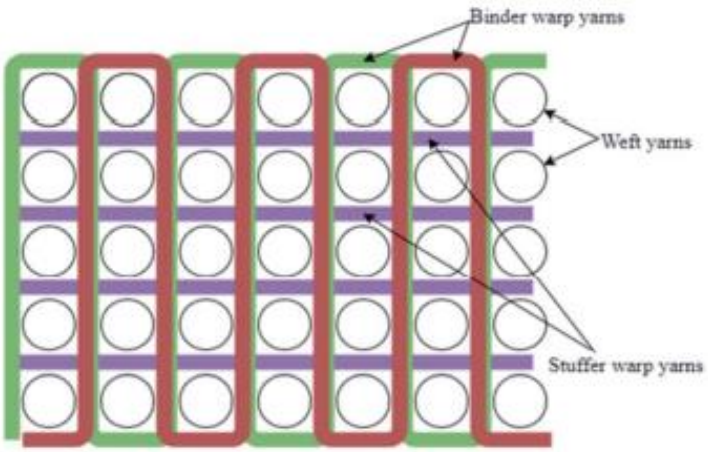

Figure 3: Basic 3D weave pattern [1]

Yarn twist, the helix angle that the individual fibers make with the longitudinal axis of the yarn also has a role in fabric performance. While too much yarn twist can cause excessive local deformation, the correct amount of yarn twist has been shown to increase the overall strength of the yarn [1, 18]. The increase in strength comes from the inward compression that the core fibers experience when the yarn is put under tension. This causes an increase in inter-fiber friction which aids in better load sharing between individual fibers.

Lastly, the orientation of the principal axes of a ply in relation to another, the number of layers used in the final layup of a soft armor, and the stitching each increase the energy absorption of the armor. Variation of the orientation between plies enhances the mechanical properties of soft armors by increasing the uniformity and increasing stab-resistance by decreasing the likelihood that an object would be able to be able to pass between parallel fibers. Increasing the number of plies also increases the energy absorption of a body armor but is typically kept between 20 – 40 layers to maintain flexibility and reduce the overall weight of the armor. Furthermore, while stitching through the ballistic fabrics does damage individual fibers and cause stress risers, research has been performed that shows that despite these negative traits, stitching effectively aids in the spread of energy from the localized point of impact to the surrounding areas [1]. This can

be witnessed in the construction of many commercially available p-aramid soft body armors that utilize diamond stitching patterns to affix the plies to one another.

3.0 Methods and Materials

3.1 Materials

The ballistic fabric to be used in this work is Kevlar 29 style 745, 3000 denier. The fabric is of a bi-directional weave with yarns 90 degrees opposed. This selection was made largely because of its ease of availability, cost, and high denier which increases its strength.

For STF preparation, fumed silica particles with an average diameter of 10 nm, silicon carbide particles and tungsten particles of diameter 80-100 nm, and super activated carbon particles with diameters less than 100 nm were procured. Because of the time and cost restraints of the project a rigorous independent study of shear thickening fluids could not be undertaken. As this was the case, the fumed silica particles were used to form a shear thickening fluid base and the other particles served as additives. This type of approach has been conducted on multiple occasions where fumed silica based STFs have shown noticeably different characteristics depending on the additive particle. It is hypothesized that the addition of silicon carbide particles, having a non-uniform geometry, will increase frictional affects between adjacent yarns and therefore decrease yarn movement. Tungsten being comparatively dense and hard to the other additives is expected to have positive effects on the energy absorption characteristics of the STF. The super activated carbon is thought to increase the amount of PEG 400 than can be held by the fabric after the intercalation process which should also have positive energy absorption qualities.

3.2 Preparation of the STF

Prior to the making of the STFs, the fumed silica particles were dried at 100°C for two hours to remove moisture and until the mass indicated on an analytical balance held constant. The STFs were prepared by fixing the total weight fraction of dispersed particles at 30%. The STFs that included an additive had the additional constituent weight fraction equal to 9%, balance fumed silica.

The particles were weighed in a large beaker and the PEG 400 was then added. As the resulting mixture was mostly large agglomerations, ethanol was then used in a 4:1 mass ratio to dilute the mixture for ease of homogenizing. The constituents were then mixed at 10,000 rpm with a rotary homogenizer for 20 minutes to ensure a uniform dispersion.

3.3 Rheological Testing

After the STFs were prepared, small samples of each were drawn and the ethanol evaporated at 100°C in an oven until the remaining mass ratio was 2:1. Agitation was required frequently to break the film that would form at the surface and prevent evaporation. A rheometer was used to perform a shear rate sweep test from 0-500s^{-1} to determine the critical and peak shear rates with a cone and plate geometry. This process was carried out by a third-party laboratory, Fluid Dynamics Inc.

3.4 Fabric Intercalation

To prepare the STF-fabric samples, the Kevlar was cut into 5-inch circles. These were then weighed and organized such that every STF mixture had multiple samples for each proceeding

test. The STFs were checked to ensure that they maintained the 4:1 ethanol to STF ratio and additional ethanol was added if needed. The ethanol in this stage of the process was to serve as a surfactant and increase the wettability of the STF. The Kevlar sheets were placed in a tray and submerged in one of the STF mixtures and were then placed in a vacuum oven to impregnate the fibers. After intercalation was achieved the oven temperature was set to 80°C to evaporate the ethanol for 1 hour. Each sample was then weighed again and compared to the initial weight to calculate and record the percent STF mass present.

3.5 Flexibility Test

A cantilever beam test was performed with the prepared sheets. One inch of the sheet was clamped to a bench and the remaining four inches were suspended over the edge. The initial drop angle was measured before a 4.7g weight was hooked on the free end of the sheet, after which the drop angle was measured again. The difference between the two measurements was recorded and is taken as a quantifier of flexibility.

Figure 4: Set up of the quasi-static test fixture using the hemispherical impactor.

3.6 Quasi-static Test

Quasi-static tests were performed on each of the STF-fabric combinations using one sheet. The test specimens were clamped in an annular vice with bolts torqued down to 90 lb-in to prevent slipping. A hemispherical, knife, and spike impactor were plunged into the fabric at a rate of

150mm/min. Three trials of the hemispherical tests were performed, while knife and spike impactors were tested once.

3.7 Dynamic Impact Test

The dynamic impact test was performed on single sheet specimens using the same annular vice from the quasi-static test and clamped with the same torque applied to the fasteners. The hemispherical impactor was mounted to a carriage of a drop tower whose total mass was recorded as 3.664 kg. Starting at a height of 20 inches a neat Kevlar sample was placed into the vice and impacted. The specimen was then replaced, and the height was incrementally increased, each time recording measurements on impact velocity and force through an oscilloscope until failure of the material was observed. This process was repeated for the remaining four STF-fabric combinations. MATLAB was used to smooth the data with Savitzky-Golay smoothing over 300 data points, plot Force-time curves, and integrate the force-displacement curves to yield Energy-time plots.

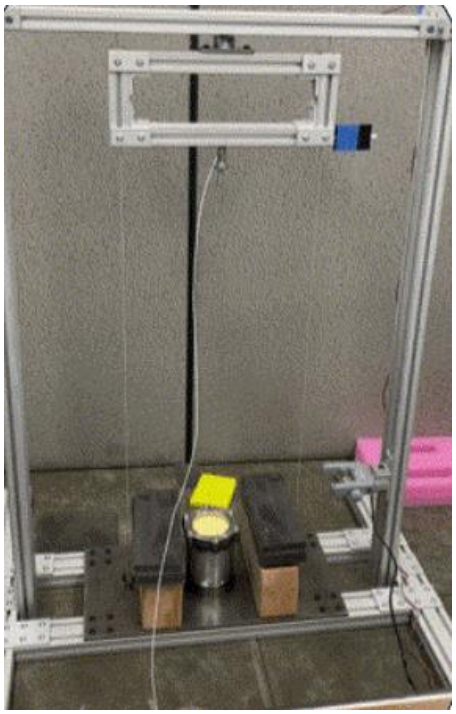

Figure 5: Image of the drop tower utilized for dynamic testing.

4.0 Results

4.1 Rheological

The results from the laboratory yielded the data in the following figures. It should be said that the STF sample containing the super activated carbon was reported to have partially solidified which was noted as being possibly due to stain hardening. The laboratory also mentioned that once the rheometer was observed to have reached maximum torque application the shear rate sweep was stopped. As such, the highest shear rate achieved during testing was $115s^{-1}$.

Figure 4 shows all of the plots of the viscosity versus shear rate, superimposed. It is clear that the three samples tested exhibit shear thickening behavior, with the tungsten additive developing the most extreme result in terms of peak viscosity.

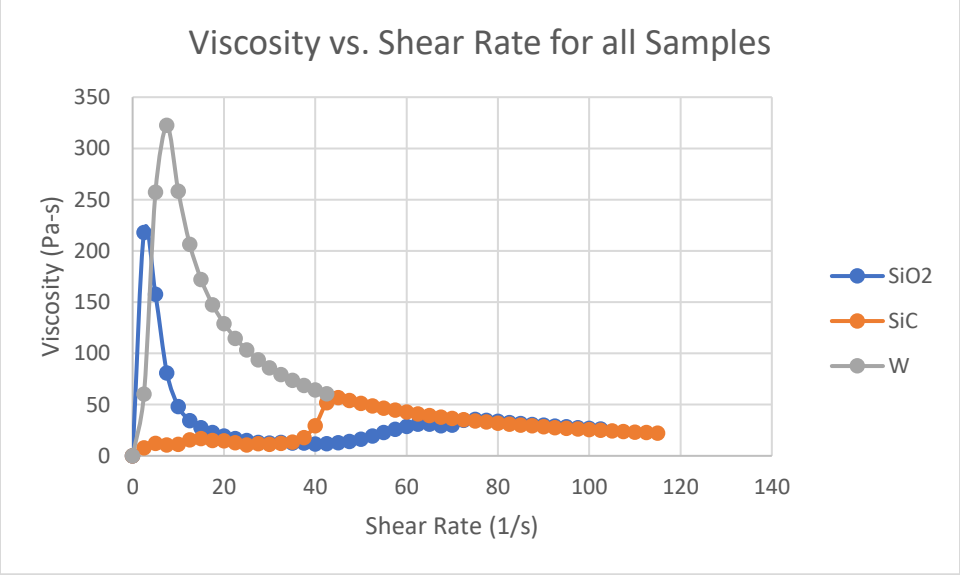

Figure 6: Plot of Viscosity versus shear rate for all samples tested (25°C)

The figures below show individual plots of viscosity versus shear rate for clarity. Referring to Figure 5 of 30 wt% SiO_2, the critical shear rate occurred at 2.5 s^{-1} resulting in a peak viscosity of 218.03 Pa-s. From Figure 6 of 21 wt% SiO_2 and 9 wt% SiC, the critical shear rate occurred at $25s^{-1}$ resulting in a peak viscosity of 57.08 Pa-s. From Figure 7 of 21 wt% SiO_2 and 9 wt% tungsten,

the critical shear rate occurred at $5s^{-1}$ resulting in a peak viscosity of 322.66 Pa-s. A summary of the results is shown in Table 1.

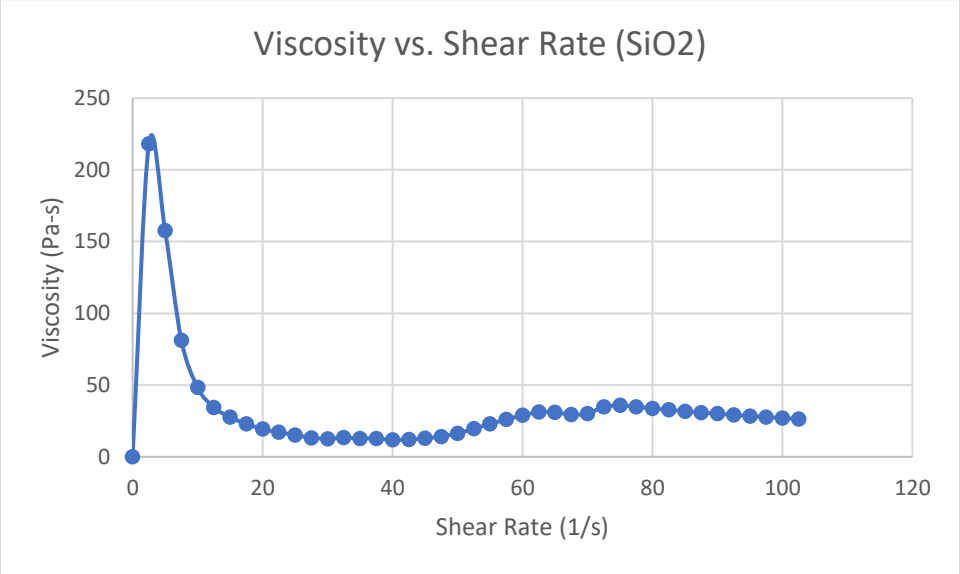

Figure 7: Plot of Viscosity versus Shear Rate for 30 wt% SiO_2.

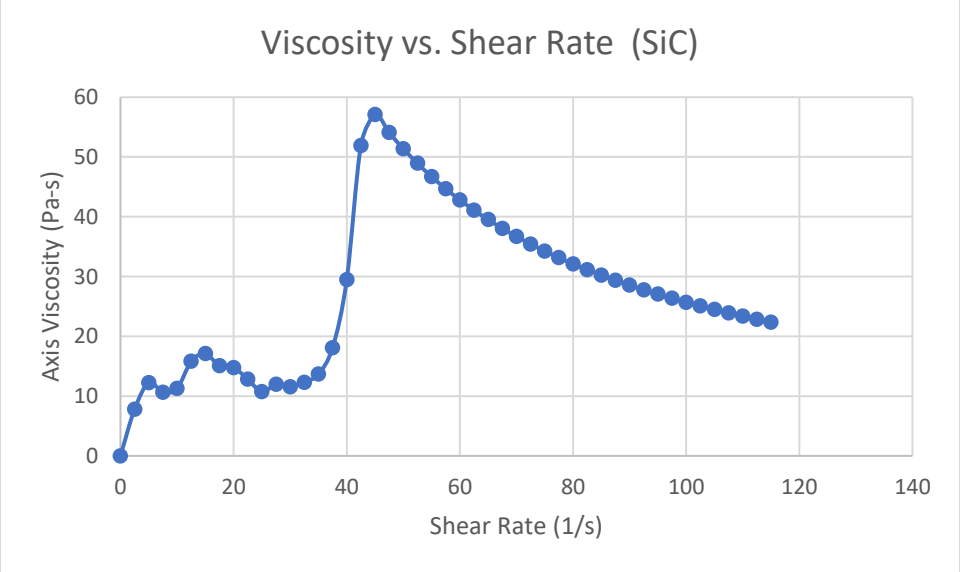

Figure 8: Plot of Viscosity versus Shear Rate for 21 wt% SiO_2 and 9 wt% SiC.

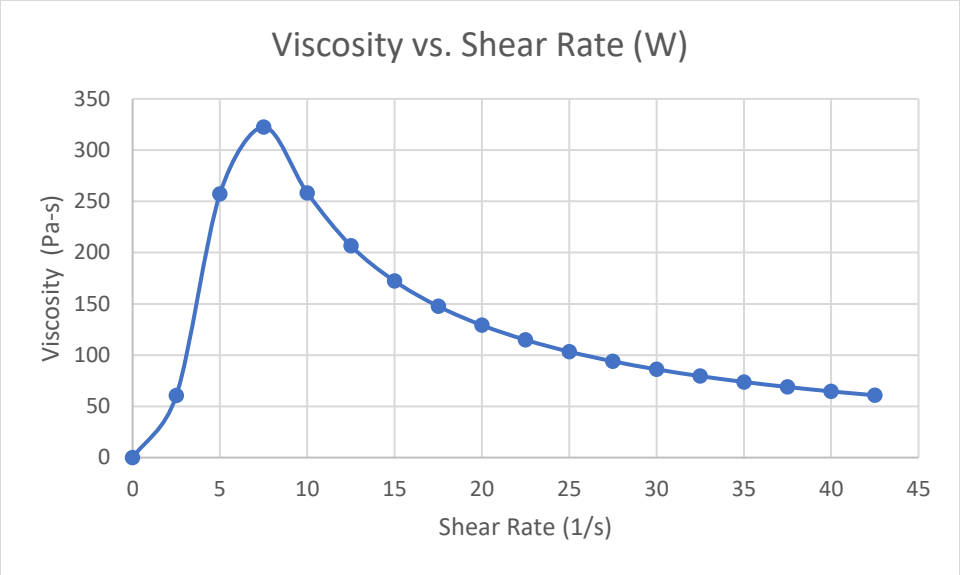

Figure 9: Plot of Viscosity versus Shear Rate for 21 wt% SiO_2 and 9 wt% SiC.

Table 1: Summary of results for initial, critical, and peak viscosity.

STF Combination	**Initial Viscosity (@2.5s^{-1}) [Pa-s]**	**Critical Shear Rate [Pa-s]**	**Peak Viscosity [Pa-s]**
SiO_2	218.03	2.5	218.03
SiO_2 + SiC	7.80	25	57.09
SiO_2 + W	60.46	2.5	322.37

[1] Initial viscosity is taken at 2.5s^{-1} as this was the first data point reported by the lab.

4.2 Flexibility

The following table shows the recorded bend angles observed from the cantilever beam test. Neat Kevlar was seen to be the most flexible with a 77° bend, SiO_2 with 63°, SiO_2+C with 58°, SiO_2+SiC with 43°, and SiO_2+W with 25°.

Table 2: Measured bend angles for each of the samples tested using a cantilever beam set up.

Sample	Neat	SiO_2	SiO_2+C	SiO_2+W	SiO_2+SiC
Bend Angle	77	63	58	25	43

4.3 Quasi-Static

Figures 10-12 show the plots of the force-displacement curves for the hemispherical, knife, and spike impactor. As expected, the hemispherical impactor encountered the greatest magnitude of forces out of three impactors, being several orders of magnitude greater. Figure 10 illustrates how the hemispherical impactor is met with continuous resistance which increases until failure.

Figure 10: Hemispherical Impactor set up.

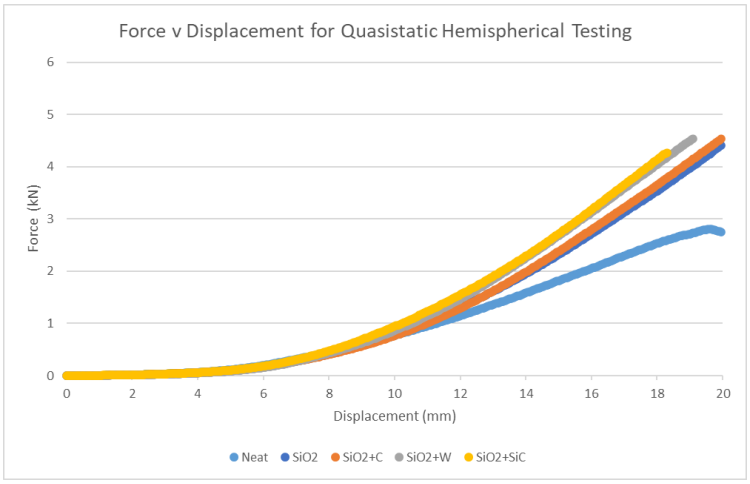

Figure 10: Plot of Force v Displacement for Quasistatic Hemispherical

It is interesting to note that the knife impactor consistently encountered lower peak forces for all materials, when compared to the spike impactor by a significant degree and resulted in a distinctly shaped plot. Each peak in Figure 11 illustrates the shearing of perpendicular fibers as the blade passes through the material.

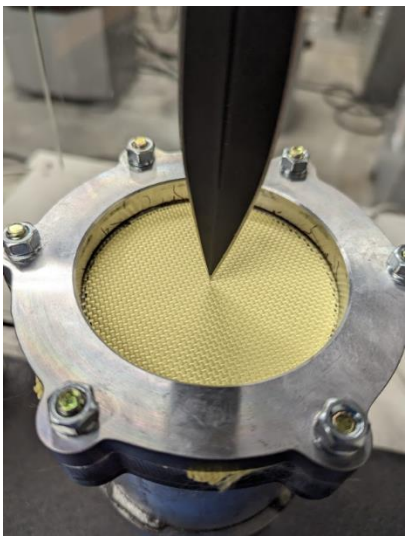

Figure 12: Knife Impactor set up.

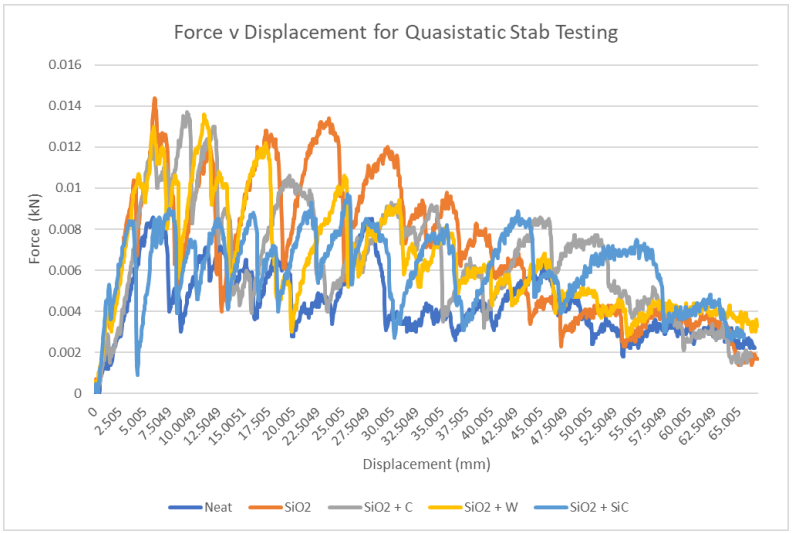

Figure 13: Plot of Force v Displacement for Quasistatic Stab Testing

Figure 12 illustrates the piecing of the spike impactor through each of the materials, with the discontinuity as seen in the 2-4mm range of displacement being the initial puncture of the tip. The force then continues to increase as the spike impactor is drawn along the tapered region of its shaft.

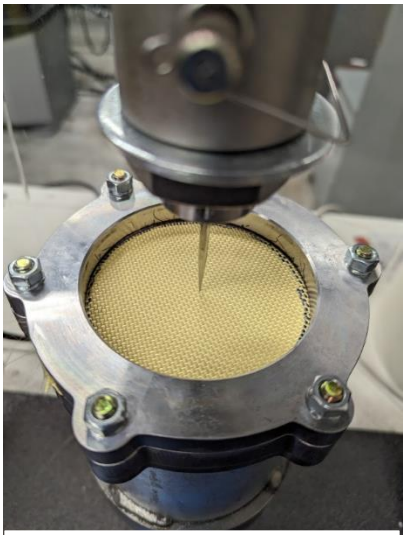

Figure 14: Spike Impactor set up.

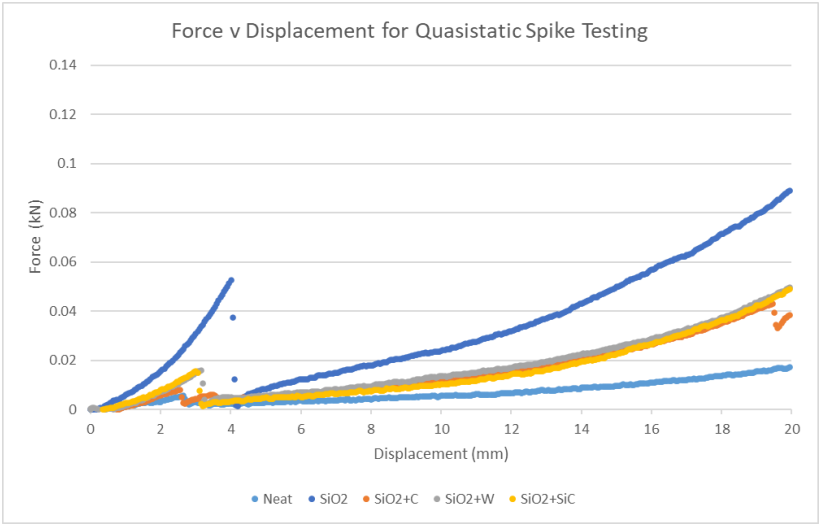

Figure 15: Plot of Force v Displacement for Quasi-static Spike Testing

Table 3: Peak force of each sample tested quasi-statically with each impactor.

Sample / Peak Force (kN)	Neat	SiO2	SiO2+C	SiO2+W	SiO2+SiC
Hemispherical	2.744	4.406	4.440	4.389	3.934
Stab	0.0086	0.0144	0.0137	0.0136	0.097
Spike	0.0207	0.1222	0.0709	0.0821	0.0941

By integrating the results of the quasistatic hemispherical force-displacement curves, the energy absorbed by the fabric can be calculated with:

$$\Delta U = \int_{A}^{B} F \cdot dx$$

Where F is the experimental force data (N), B and A are the upper and lower limits of the experimental force data, and dx is the step of the displacement (m). Force-displacement data is cutoff at negative values and at peak force. Applying the data gathered from the average of three trials, the following can be concluded:

Table 4: Summary of results for average integral energy of each sample.

Sample	Average Integral Energy (J)
Neat	20.51
SiO2	20.03
C	24.17
W	23.23
SiC	19.32

Additionally, the initial and late stiffnesses of the samples can be calculated. These values were obtained from the average slope of two quasistatic hemispherical trials. Initial stiffness values were measured between ~0.5mm and ~2mm of deflection, while the late stiffnesses were calculated between ~10mm and ~17mm of deflection.

Table 5: Summary of results for average initial and late stiffness of each sample.

Sample	Neat	SiO2	SiO2+C	SiO2+W	SiO2+SiC
Average Initial Stiffness (N/mm)	0.468	0.485	0.467	0.395	0.415
Average Late Stiffness (N/mm)	10.21	17.45	18.70	19.85	19.40

4.4 Dynamic Impact

As used in this section, “failure” and “onset of failure” are referred to interchangeably. During the impact test it was noted that slipping of the material near the edge of the vice was occurring to a small degree, preventing the complete rupture of the fibers or

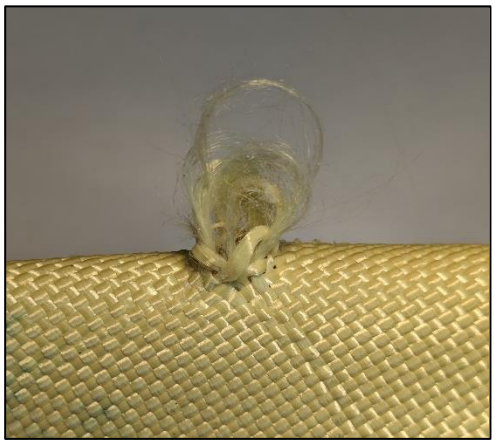

Figure 11: Image of localized fiber pull-out.

complete failure as can be seen in Figure 13. As such, the failure criterion was designated to be that of fiber pull out or the onset of failure.

Based on Figure 14, which is representative of all samples tested, the onset of failure is qualified by the plateau region following the peak force which can be explained by fiber pullout as well as an increase in impact duration. Figure 15 summarizes the peak forces encountered at the impact heights where the onset of failure is observed for the tested samples. Neat Kevlar is seen to fail at 23 inches with a peak impact force of 2219N. All other STF-fabric combinations

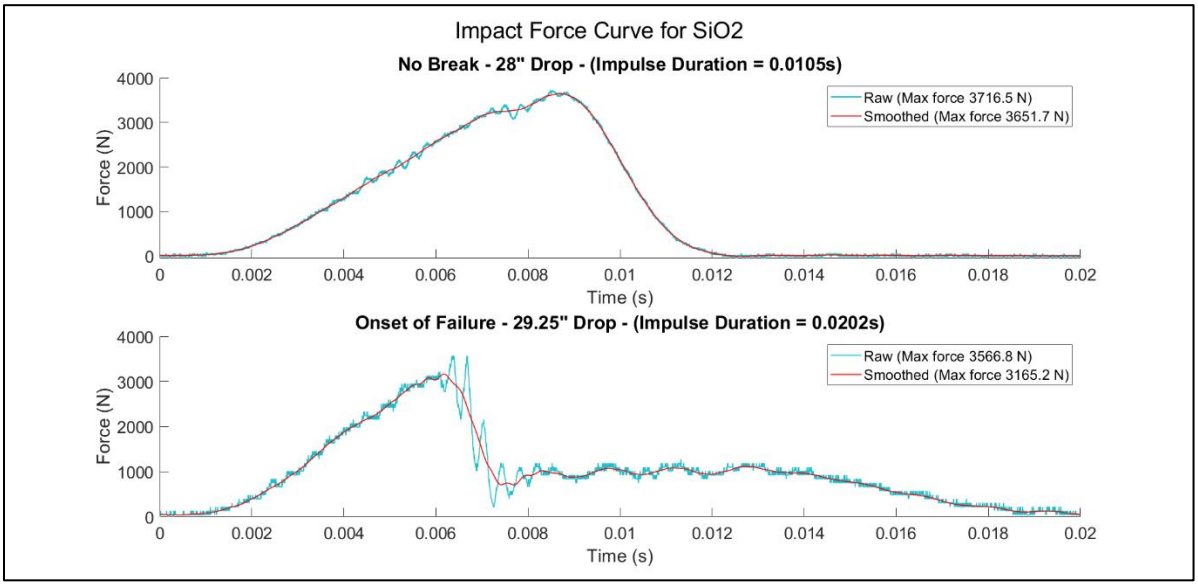

Figure 17: Force curves showing comparison between no failure and the onset of failure for SiO_2.

fail at 29.25 inches with the SiO_2 sample encountering a peak force of 3165N, SiO2+C at 3018N, SiO_2+W at 3116N, and SiO_2+SiC at 3494N.

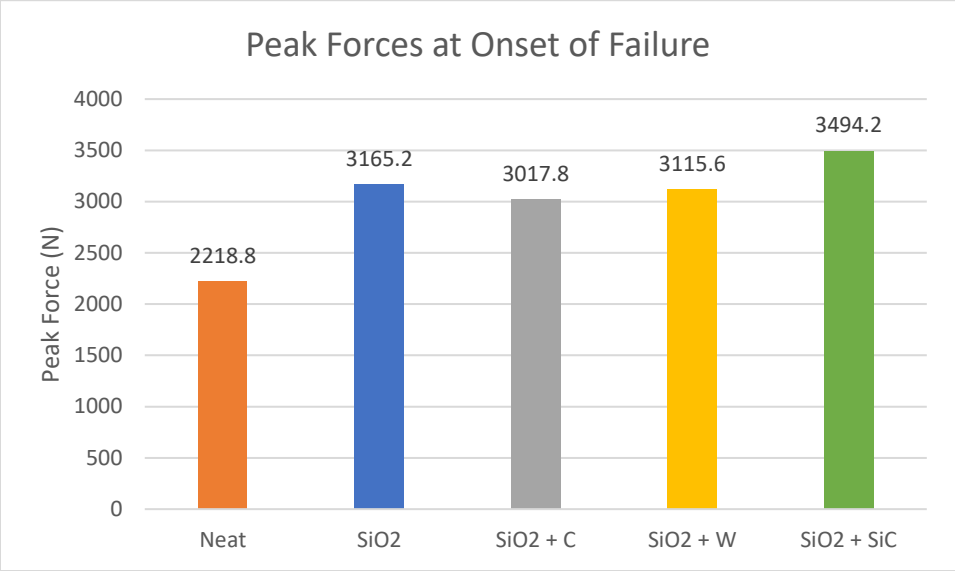

Figure 18: Chart of peak forces at the onset of failure.

From Table 8, the impulse durations leading up to the onset of failure are compared to neat Kevlar. Observing the data at the failure heights, neat Kevlar has an impulse duration of 0.0124 seconds while SiO2, SiO2+C, SiO_2+W, and SiO_2+SiC have impulse durations of 0.0202, 0.0137, 0.0146, and 0.0233 seconds respectively.

Table 6: Impulse duration before and after the onset of failure.

Impulse Duration Before and After Onset of Failure						
STF		$Neat$	SiO_2	$SiO_2 + C$	$SiO_2 + W$	$SiO_2 + SiC$
No Break	Height(in)	22.125	28	28	28	28
	Impulse Time (s)	0.0122	0.0105	0.0108	0.0113	0.0126
Onset of Failure	Height(in)	23	29.25	29.25	29.25	29.25
	Impulse Time (s)	0.0124	0.0202	0.0137	0.0146	0.0233

Referring to Table 9, the magnitude of the energy absorption is correspondingly greater for the STF-fabrics, at the onset of failure, however, the percentage of energy absorbed through plastic deformation was systematically lower compared to neat Kevlar.

Table 7: Energy absorbed by the fabrics for each drop height.

Energy Absorbed by Fabric						
Drop Height (in)	Theoretical Impact Energy (J)	Energy Absorbed (J) [% Energy Absorbed]				
		$Neat$	SiO_2	$SiO_2 + C$	$SiO_2 + W$	$SiO_2 + SiC$
22.125	20.2	17.6 [87.2%]				
23	21.0	20.6 [98.1%]	17.3 [82.2%]	17.7 [84.3%]	17.6 [83.8%]	17.0 [80.9%]
24	21.9	20.6 [93.8%]				
26	23.7	23.2 [97.7%]				
28	25.6		20.7 [81.0%]	21.6 [84.5%]	22.8 [89.1%]	23.5 [91.7%]
29.25	26.7		22.5 [84.4%]	24.8 [92.8%]	24.7 [92.4%]	23.9 [89.6%]
33	30.1		28.9 [96.0%]	27.8 [92.1%]	28.4 [94.3%]	23.9 [79.4%]

5.0 Discussion

The STF viscosity curves are mostly consistent with the findings from other previous results of fumed silica based STFs. All curves possess a sharp increase in viscosity at a relatively low shear rate and exhibit a shear thinning phase afterwards. Normally, the shear thickening spike would be preceded by another shear thinning phase. This is only vaguely apparent in the case of the SiO_2 + SiC sample. However, as the resolution of data acquisition was limited in this test, it is possible that this characteristic region occurred within a narrow range of shear rates between 0-2.5s^{-1}.

While it was expected the increased density of the additive particle would also increase the viscosity of the STF due to a greater volume packing fraction, the opposite is observed in the case of SiO_2 + SiC. The exact cause of this is unknown, but it is surmised that it is due to the fact the SiC does not form a shear thickening solution with PEG400 on its own. As such, the dispersed SiC particles interrupt the SiO_2 hydro clusters in such a way that decreases their overall size, as compared to the STF made only of SiO_2, and effectively diminishes the shear thickening effect.

On the other hand, the solution containing tungsten shows the opposite effect. Where the peak viscosity is over 1000% higher than the SiO_2 STF. It is suspected that this is due to the extremely high density of the tungsten particles. Whereas the bulk density of the SiC particles is .05 g/cm^3, the bulk density of the tungsten particles is 4.1 g/cm^3, which is 82 times greater. While the tungsten particles may intrude into the SiO_2 hydro clusters in the same manner as SiC, the number of particles in solution is far fewer and may not have a such a widespread effect on limiting the size of the SiO_2 hydro clusters. This, and their more uniform spherical shape may serve to enhance the shear thickening effect in some manner. Alternatively, it is possible that the tungsten

particles can form a STF with PEG400 on their own, and the combination of two shear thickening particles compounds.

The results of the SiO_2 + W combination are most promising, although the low critical shear rate may be a concern. With the peak viscosity occurring at such a low shear rate, the STF could impede movement and flexibility when intercalated into a ballistic fabric for the use in body armor. This is further highlighted when observing the results from the cantilever beam test where the tungsten STF also possesses the least bend angle.

Quasistatic Testing

Results from trials conducted with the hemispherical impactor showed initial stiffness calculated was similar across all materials, though it was interesting to note that the neat Kevlar tests did not have the lowest initial average stiffness. Additional testing may need to be conducted confirm whether these results are consistent, but the similar results were mostly expected as the low velocity of the Instron machine was meant to simulate a procedure that would not activate the shear thickening properties of the STF. On the other hand, late average stiffness for all STF-infused samples had at least a 70% minimum increase compared to the neat samples. As mentioned before, the STF was not expected to activate during this experiment. Thus, the increase in stiffness should be attributed more towards the STF acting as an adhesive within the gaps of the STF fibers that binds the sample together further.

Both experiments involving the knife and spike impactor did not give any data relevant to the properties of the material due to how failure occurred too suddenly and at such a low force. When analyzing Figures 11 and 12 from the measured data, only a few assumptions and theories were implied from the curve and sample. Unlike the hemispherical impactor, the knife impactor

was able to slice through the sample with no obstruction, meaning failure was immediately observed. The recorded forces were jagged and sudden as the displacement increased; however, these forces are extremely low in magnitude. These results are likely due to the knife continuously cutting through the fibers, with each peak representing a different fiber that was tensioned and eventually cut. Similarly, the experiments using the spike impactor also failed immediately, with the force measured gradually rising after failure. This increase can be attributed to the widening of the impactor as it traveled vertically downwards, placing the surrounding fibers in increasing tension, but not being able to slice through like the knife impactor.

Dynamic Testing

While the results of the dynamic testing do show promising trends, it is important to address the limited testing that was performed before proceeding. Due to time and material limitations dynamic testing was only performed once for each drop height and thus the data provided is to be considered preliminary. Furthermore, since fabric slipping was observed within the clamp and localized fiber pullout prevented complete fiber failure, much of this data is largely a reflection on the performance of the clamping method rather than the fabric itself. From analysis of the tested samples, it is apparent that the fabrics likely would have been able to outperform the results achieved if the perimeter of the fabric was sufficiently constrained.

What can be said is that the treatments performed on the fabrics had a net benefit on the energy absorbing characteristics of all of the STF infused fabrics. While the neat fabric failed at a drop height of 23”, each STF infused sample consistently failed at a drop height of 29.25”. Similarly, there is a 36% - 57% increase in the measured peak force at the onset of failure for the infused fabrics when compared to the neat counterpart. Unfortunately, while improvements were observed in the fabric, it remains unknown if these effects are due to the shear thickening nature

of the fluid infused within the fabric or largely driven by the increased inter-fiber friction due solely from the addition of the nanoparticles. Based on the rheological data, it was predicted that the $SiO_2 + W$ sample would perform the best since the fluid's viscosity is the highest at the expected shear rate within the fabric during the dynamic testing. However, after the dynamic testing, it was found that the performance of the $SiO_2 + W$ fabric was indiscernible to the other infused fabrics with much lower viscosity fluids. This suggests that the energy absorption of the fabric in this case is dependent upon the addition of the particles rather than shear thickening, and further testing would be necessary to definitively determine which mode is responsible for the observed performance increase.

Additionally, it is important to note that dynamic testing was not conducted for the knife nor spike indenters. This was largely due to the fact that the forces found to pierce the fabrics during quasistatic testing were relatively low and concern developed for whether or not useful data could be derived from the small drop heights that would be necessary. In this case, it would likely work best to stack multiple layers of fabric to increase the required drop height and impact force, but since the clamping fixture was designed to clamp only one layer of fabric, its ability to hold multiple layers would likely be limited.

Comparisons were also drawn between the energy absorption results of both the quasistatic and dynamic impact experiments. Neat Kevlar had a consistent result of around 20.5 Joules, which was expected and showed that differences in the later STF results would be a constituent of the material itself, not the test setup. On the other hand, both $SiO2$ and $SiO2 + W$ had an increased absorbed energy in the dynamic impact test compared to the quasistatic test, though the magnitude of increase is relatively minor. Although this increase implies an increase in ability to absorb

energy with the added STF, more testing is required in order to conclude if this is benefit is a result of the shear thickening properties.

6.0 Future Works

Future works may choose to investigate these same STF compositions under a more precise range of shear rates, particularly in the low range to observe the occurrence of the shear thinning phase prior to the critical shear rate. Additional experimentation should also be conducted with SiC additives to determine, with more certainty, the cause of its reducing effect in terms of shear thickening behavior. Adjusting particle size to mimic that of the fumed silica as well as controlling the particle geometry may provide more insight on the matter. A similar approach to the tungsten STF should also be undertaken for the same purpose.

Improvements to the clamping method should also be made to eliminate any slipping effect as was observed in the above experimentation. Additional bolts or protrusions on the clamping faces of the vice could be used to alleviate this issue.

The quasi static and dynamic impact test should also be performed over a larger number of samples to obtain more precise data and decrease uncertainty. These same tests should also be repeated using Newtonian fluids as the stiffening effect observed during quasi static conditions and the increase in energy absorption observed during the dynamic impacts cannot be attributed to the STF or particle frictional effects with certainty. The dynamic tests should also be performed according to shear rate instead of impact height and velocity. This would allow the comparison of the STF-fabric's impact response to the viscosity curves.

A V_{50} ballistic test, following MIL-STF-662F is also necessary to determine the feasibility for these materials to be used as a foundation for a new level III body armor. In preparation for this test, consideration to the physical design of the soft body armor must be given. Weave patterns, fiber material, stitch pattern, and composite materials should be experimented with in order to better ascertain the most efficient energy absorber and dissipator. Additionally, by focusing on the

physical aspect of the body armor, the effects of excessive stiffness and/or low critical shear rate may shed light on its practicality as a useable piece of equipment.

References

[1] Elizasturgill. (n.d.). *Elizasturgill*. ATEK Defense Systems. Retrieved June 16, 2022, from https://atekdefense.com/nij-body-armor-threat-levels-summary-0101-06-standard/

[2] Mawkhlieng, U., Majumdar, A., & Laha, A. (2020). A review of fibrous materials for soft body armour applications. *RSC Advances*, *10*(2), 1066–1086. https://doi.org/10.1039/c9ra06447h

[3] *Best body armor plates: Body armor plates*. Safe Life Defense. (2022). Retrieved June 22, 2022, from https://safelifedefense.com/product/fras-plate-flexible-rifle-armor-system/

[4] Cwalina, C. D., McCutcheon, C. M., Dombrowski, R. D., & Wagner, N. J. (2016). Engineering enhanced cut and puncture resistance into the thermal micrometeoroid garment (TMG) using shear thickening fluid (STF) – armor™ absorber layers. *Composites Science*

[5] *Versa level 3+ flexible body armor 10"x 12"*. Guard Dog Body Armor. (2022, June 8). Retrieved June 22, 2022, from https://gdbodyarmor.com/product/versa-level-3-flexible-body-armor-10x12/

[6] Zarei, M., & Aalaie, J. (2020). Application of shear thickening fluids in material development. *Journal of Materials Research and Technology*, *9*(5), 10411–10433. Htt ps://doi.org/10.1016/j.jmrt.2020.07.049

[7] Wang, Y. (2016). *Ballistic Body Armour Using Shear Thickening Fluids For Enhancing Stab Resistance* (thesis). UoM, Manchester.

[8] Eric, Dr & Wetzel, D & Norman, Prof & Wagner, Norman & Lee, Young & Egres, Ron & Kirkwood, Keith & Kirkwood, John. (2003). Advanced body armor utilizing shear thickening fluids.

[9] Wei, M., Lin, K., & Sun, L. (2022). Shear thickening fluids and their applications. *Materials & Design, 216*, 110570. https://doi.org/10.1016/j.matdes.2022.110570

[10] Hoffman, R. L. (1998). Explanations for the cause of shear thickening in concentrated colloidal suspensions. *Journal of Rheology*, *42*(1), 111–123. https://doi.org/10.1122/1.550884

[11] Ball, R. C., & Melrose, J. R. (1999). Shear thickening in colloidal dispersions. *AIP Conference Proceedings*. https://doi.org/10.1063/1.58445

[12] Olsson, P., & Teitel, S. (2007). Critical scaling of shear viscosity at the jamming transition. *Physical Review Letters*, *99*(17). https://doi.org/10.1103/physrevlett.99.178001

[13] Mari, R., Seto, R., Morris, J. F., & Denn, M. M. (2014). Shear thickening, frictionless and frictional rheologies in non-Brownian suspensions. *Journal of Rheology*, *58*(6), 1693–1724. https://doi.org/10.1122/1.4890747

[14] Wagner, N. J., & Brady, J. F. (2009). Shear thickening in colloidal dispersions. *Physics Today*, *62*(10), 27–32. https://doi.org/10.1063/1.3248476

[15] Mawkhlieng, U., & Majumdar, A. (2020). Designing of hybrid soft body armour using high-performance unidirectional and woven fabrics impregnated with shear thickening fluid. *Composite Structures, 253*, 112776. https://doi.org/10.1016/j.compstruct.2020.112776

[16] Kalman, D. P., Merrill, R. L., Wagner, N. J., & Wetzel, E. D. (2009). Effect of particle hardness on the penetration behavior of fabrics intercalated with dry particles and concentrated particle−fluid suspensions. *ACS Applied Materials & Interfaces*, *1*(11), 2602–2612. https://doi.org/10.1021/am900516w

[17] Egres, R. G., Decker, M. J., Halbach, C. J., Lee, Y. S., Kirkwood, J. E., Kirkwood, K. M., Wagner, N. J., & Wetzel, E. D. (2006). Stab resistance of shear thickening fluid (stf)–kevlar

composites for body armor applications. *Transformational Science and Technology for the Current and Future Force*, 1–20. https://doi.org/10.1142/9789812772572_0034

[18] Yang, H. H. (1993). *Kevlar Aramid Fiber*. J. Wiley.

[19] Utracki, L. A. (2010). Rigid ballistic composites. *NRC Publications Archive*, 1–78. https://doi.org/10.4224/16885314